

### Landslide hazard levels analysis considering displacement traction

Xingchi Chen<sup>1,\*</sup>, Yuzhi Meng<sup>⊠1,\*</sup>, Junzhe Zhou<sup>1</sup>, Yutao Zhou<sup>2</sup>, Zhengdong Leng<sup>3</sup>, Kun Wang<sup>3</sup>

- 1. School of Smart City, Chongqing Jiaotong University, Chongqing 400074, P. R. China
- 2. Chongqing Chuandongnan Engineering Survey & Design Institute Co., Ltd., Chongqing 401120, P. R. China
- 3. China Gezhouba Group Expl Co., Ltd., Hunan 410000, P. R. China
- ⊠: Corresponding author, mengyuzhi@mails.cqjtu.edu.cn

**Abstract:** Accurately assessing the hazards posed by landslides is of great importance for disaster prevention and mitigation. This study proposes a method of landslide hazard levels analysis based on displacement traction, a term referring to the correlated directional influence between surface displacement vectors at GNSS (Global Navigation Satellite System) monitoring points. By analyzing these spatial correlations, the optimal grid unit size is determined for refined hazard levels assessment. To construct a representative target area, the improved Sparrow Search Algorithm was combined with the k-means clustering algorithm, integrating displacement characteristics and the derived grid unit size. A hazard assessment dataset was then developed for the target area. Subsequently, a stacking ensemble model was employed to evaluate landslide hazard levels using eleven influencing factors, including surface roughness, elevation, and slope angle. Experimental results demonstrated that the proposed method outperformed the conventional fixed-grid approach, yielding a 2.15% improvement in overall accuracy, a 1.30% increase in F1-score, and a 3.75% gain in the kappa coefficient. This study not only enriches the theoretical foundation of assessing landslide hazard levels but also provides a powerful technical support and practical guidance for the scientific prevention and control of landslide disasters.

<u>**Keywords:**</u> displacement traction; k-means algorithm; landslide hazard levels

#### 1 Introduction

Landslides represent a major geological disaster seriously threatening human lives and infrastructure constructions<sup>[1]</sup>. Thus, the assessment of landslide hazard levels has become an indispensable part of prevention and mitigation of landslides<sup>[2]</sup>. The analysis of landslide hazard levels is gradually being shifted geological investigations from traditional simulations to advanced remote sensing and geographic information systems. Many landslide monitoring projects have been conducted using Lidar and InSAR (Interferometric Synthetic Aperture Radar), which can provide accurate surface displacement data<sup>[3-5]</sup>. Despite their wide-area capabilities, both Lidar and InSAR suffer from limitations such as low temporal resolution, noise interference in vegetated or steep-slope areas, and difficulty detecting localized deformation near failure thresholds, which restrict their effectiveness for fine-scale hazard analysis. However, despite their effectiveness in monitoring landslide hazards across large areas, these methods fall short in terms of refined individual landslide hazard levels analysis, particularly regarding correlations between displacement vectors at various monitoring points. In

<sup>\*</sup>These authors contributed equally

landslide hazard level research, the displacement traction effect describes how the surface movement at one monitoring point can influence the movement at adjacent points. By analyzing surface displacement data from multiple monitoring points, the correlation between displacement vectors can be identified. Such analysis is crucial for predicting and preventing landslides.

In addition to modeling physical processes, the choice of spatial analysis units—especially the grid size—plays a crucial role in landslide hazard mapping. Several studies have shown that inappropriate grid size may obscure critical spatial variability or introduce excessive noise, leading to inaccurate susceptibility or hazard classifications. For instance, Süzen and Doyuran compared grid-based versus slope unit-based approaches and found significant differences in model performance depending on grid resolution<sup>[6]</sup>. More recently, Reichenbach et al. reviewed over 150 landslide susceptibility models and concluded that no standard grid size can be universally applied; instead, scale optimization should be tailored to each case study area<sup>[7]</sup>. These findings underscore the need for adaptive grid size determination in landslide modeling.

For individual landslides, grid unit delineation constitutes an important part of hazard level analysis. Traditional methods usually rely on empirical delineation, which often depends on fixed map scales or expert judgment, lacking quantitative optimization and overlooking localized deformation—leading to inaccurate or overly generalized assessments. Li et al. [8] developed an empirical formula for calculating the grid unit size according to the scale of topographic maps. However, the selection of the grid unit size required more thorough study as it could greatly affect the accuracy of landslide hazard levels assessments [9,10].

Acknowledging this fact, this research proposes a new methodology, which considers the displacement traction effect, to analyse landslide hazard levels. It is focused on a single landslide. The size of the optimal assessment unit is objectively determined through an in-depth cluster analysis of the characteristics of displacement vectors at the GNSS (Global Navigation

Satellite System) monitoring points. The grid units, where the monitoring points are located, are divided into different hazard levels based on their displacement characteristics, upon which an accurate assessment dataset is constructed. Because the traditional k-means clustering algorithm tends to converge to a local optimum, the proposed methodology integrates the improved sparrow search algorithm (ISSA), effectively enhancing global search capabilities and clustering. Moreover, to overcome the limitations of using a single classification model in the assessment of landslide hazard levels[11-13], which is complex by nature, the proposed methodology employs an integrated learning strategy, specifically, a stacking integration model<sup>[14]</sup> that combines the advantages of multiple strong classifiers into a multi-level classifier<sup>[15]</sup>, achieving the significantly higher accuracy of hazard levels assessment in comparison with the single classification models<sup>[16,17]</sup>.

#### 2 Research methods

## 2.1 Determination of grid unit size based on displacement traction

The selection of the grid unit size significantly affects the assessment of landslide hazard levels. In the hazard assessment of a single landslide, each grid unit represents a specific spatial area and is assigned with a set of geographic attributes such as elevation, slope angle, and lithology. Theoretically, the data attributes within each grid unit should be consistent. Although regular grid units are most commonly used, their sizes are typically determined empirically or based on the fixed formulas. If the grid unit size is too large or too small, it can disrupt data consistency, leading to inaccurate assessment results. Therefore, this research focuses on determining the optimal grid unit size based on the correlation characteristics of monitoring points. Specifically, displacement data from GNSS monitoring points are combined to form a target area for cluster analysis. The optimal grid unit size is determined by considering the displacement direction and ensuring the consistency in the correlations between monitoring points.

First, based on an empirical formula<sup>[18]</sup>, a coarse division into regular grids is performed. By calculating the error range of the formula, a preliminary range of a grid unit size is obtained:

$$G = 7.49 + 6 \times 10^{-4} \times M - 2 \times 10^{-9} \times M^2 + 2.9 \times 10^{-15} M^3$$
 (1)

where G is the grid unit size, and M is the topographic map scale. Then, the optimal grid unit size is established by incorporating the displacement traction. To analyze the directional characteristics of surface displacement, a local Cartesian coordinate system is defined for each monitoring point, with the monitoring point itself as the origin. The displacement trajectories of the monitoring points are categorized according to the four quadrants of the coordinate axes (I, II, III, and IV) to obtain the distribution of the displacement trajectories of the monitoring points (Figure 1). The consistency of the displacement direction in each grid unit is evaluated by calculating the trajectory classification results of the displacement characteristics of all monitoring points in that grid unit. The consistency of the displacement direction in each grid unit is also quantitatively evaluated to generate a consistency rate. A grid unit is considered to have the optimal size if the displacement direction consistency rate of all monitoring points is high.

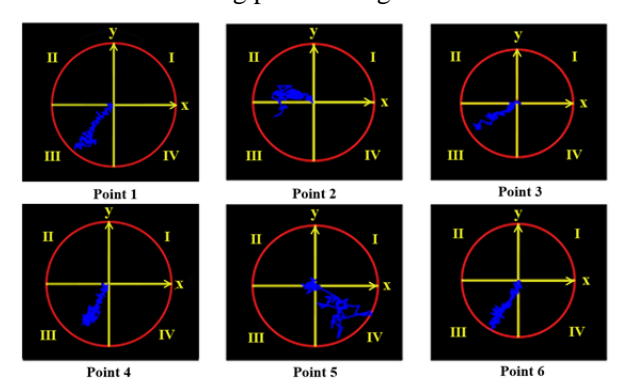


Fig. 1 Displacement trajectories of GNSS monitoring points 1–6

#### 2.2 Target area construction

Based on the optimal grid unit size, the target area for hazard level assessment is constructed using the

proposed clustering approach. However, due to the limited number of GNSS monitoring points typically available for a single landslide event, sample data expansion is necessary to ensure sufficient spatial coverage and statistical consistency within each grid unit. To this end, a semisupervised learning strategy is introduced to augment the displacement-derived features extracted from GNSS data and improve the robustness of the clustering process. The Improved Sparrow Search Algorithm (ISSA) is subsequently employed to optimize the k-means clustering. Through this displacement feature cluster analysis, the target area is combined with the optimal grid unit size to form a hazard assessment sample set.

#### 2.2.1 Sample data expansion

As the limited number of GNSS displacement monitoring points in a single landslide cannot meet the requirement for directionally consistent statistical data under the same grid unit size, the semisupervised learning approach is used to expand the labeled samples. Multiple random points are generated as the unlabeled sample data and then combined with the labeled data, which consist of the detection points associated with displacement direction labels. Semisupervised learning is then used to transfer the labels to the random points, resulting in a significantly expanded labeled dataset.

#### 2.2.2 Target region construction

The expanded labeled dataset must be effectively used to construct the target area for analysing landslide hazard levels. To rationally organize the data for accurately reflecting the actual hazard posed by a landslide, the k-means clustering algorithm, a widely used method in cluster analysis for data mining due to its simplicity and efficiency<sup>[19]</sup>, is employed to integrate the displacement-derived features into the target regions with clear hazard labels. Its core objective is to assign each sample point to the cluster that corresponds to the nearest cluster center after their similarity to each center (e.g., Euclidean distance). However, the k-means algorithm relies on the initial solution and is prone to

converging to a local optimum, which reduces its ability to obtain globally optimal clustering results. To overcome this limitation, a new type of swarm intelligence optimization algorithm is structured by further integrating with ISSA. Its key lies in simulating the foraging and social behaviors of sparrows. The core optimization achieved by ISSA succeeds by means of introducing adaptive fractional-order calculus to enhance the sparrow search process by adjusting the trajectory update mechanism and thereby improve the convergence accuracy compared to the standard SSA<sup>[20]</sup> (Figure 2). The k-Means clustering combined with ISSA can determine the global scope of optimization in the search process, effectively improving clustering performance. Specifically, this approach enables the clustering of characteristic data of displacements from a group of monitoring points. The results are then combined with the optimal grid unit to obtain target regions and construct a sample dataset for each target region based on the assessed landslide hazardousness.

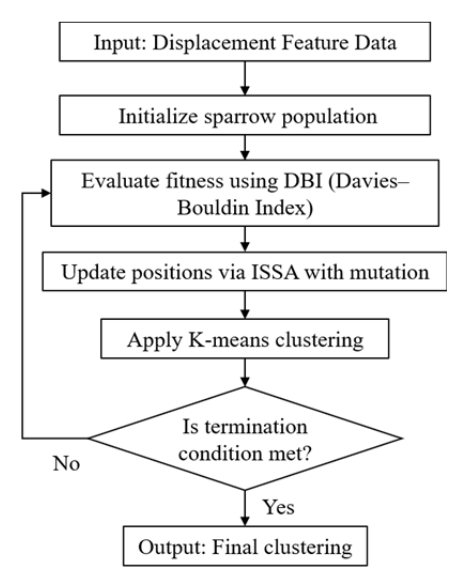


Fig. 2 Flowchart of the ISSA combined k-means clustering

## 2.2.3 Construction of landslide hazard classification model using ensemble learning

The assessment of landslide hazard levels can be considered a classification and prediction problem. The accuracy of the results positively correlates with the classification performance. To improve the predictive

accuracy, an integrated learning framework is implemented by combining multiple base classifiers. Specifically, we compare and evaluate the performance of several commonly used models, including Logistic Regression, Gaussian Process, Decision Tree, Support Vector Machine (SVM), Random Forest, and Extreme Gradient Boosting (XGBoost). Due to the limitations of individual classifiers when dealing with sparse, imbalanced, noisy, and/or high-dimensional data<sup>[21-25]</sup>, a stacking ensemble strategy is further employed to take advantage of their strengths and enhance the overall classification performance.

Among these multi-classifier systems, proposed methodology employs a stacking integration model as shown in Figure 3. The stacking algorithm has a multilayer structure in general. To avoid overfitting, a streamlined two-layer design is adopted with using a meta-learner that is simpler than the base learners in the first layer in order to maintain satisfactory generalization performance. The stacking method is essentially a classification based on labels. So, the meta-learner is used to model the relationships between the labels and the corresponding influencing factors. Multiple strong learners are trained on the constructed dataset. Then, the one with the highest classification accuracy is chosen as the first-level learner. Based on this, various meta-learners are trained. and the performance of different learner combinations is evaluated on both the training and test datasets. Since the prediction attempted in this research is a classification problem, the simplest and most accurate meta-learner is selected.

#### 3 Experimental procedures

#### 3.1 Target area construction

The area under study is Guang'an Village in Dahe Township, Wuxi County, Chongqing, China, at about 31.54° N, 109.61° E. On October 21, 2017, a rapid large-scale landslide occurred in this area, resulting in nine casualties. With a total volume of approximately  $6 \times 10^6$  m<sup>3</sup> of earth, this landslide generated a significant accumulation of earth and rock

debris, severely affecting buildings, transportation, and especially the water supply system. Due to its large scale, it caused different degrees of deformation on both sides of the slope, resulting in the formation of different impact zones. Satellite images over the area before and after the landslide are shown in Figure 4.

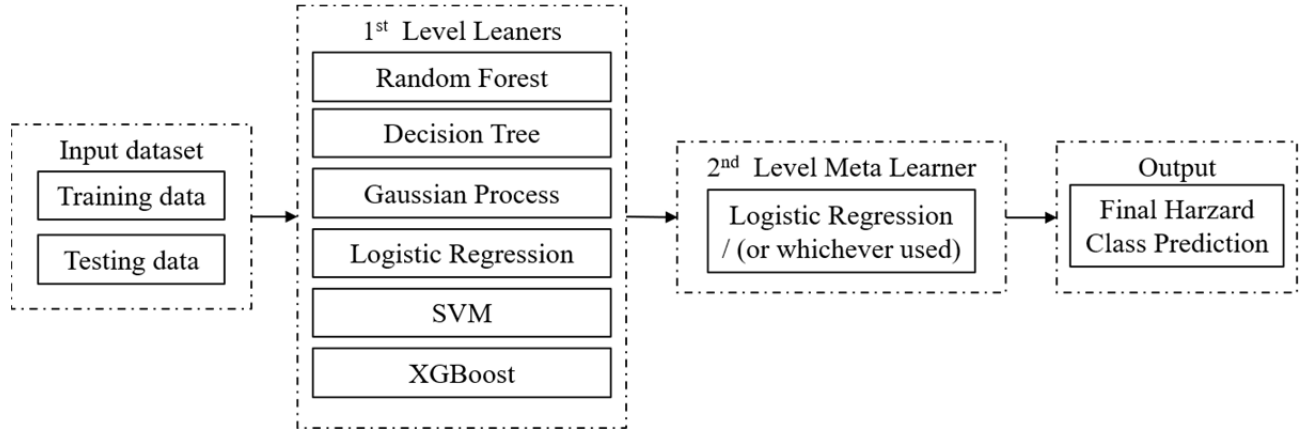


Fig. 3 Two-Layer Stacking Framework

Rainfall is one of the main factors affecting landslides. The Guang'an area has typical subtropical monsoon climate, with high temperature and abundant concentrated precipitation in summer. As shown in Figure 5, the period between September and October 2017 was characterized by continuous rainfall with the maximum daily precipitation exceeding 1300 mm.





Fig. 4 Satellite images before and after the landslide

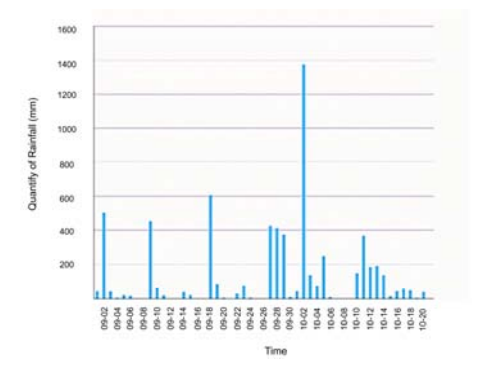


Fig. 5 Histogram of rainfall in Guang'an area (2017/09/02-2017/10/20)

#### 3.2 Cluster analysis of displacement data

#### 3.2.1 Grid Unit Scaling and Sample Expansion

After the empirical formula (1), with a topographic map scale of 1:2000, the preliminary grid unit size was approximately  $9 \times 9$  m<sup>2</sup>. The optimal grid unit size after integrating the error range of the formula became in the range of  $5 \times 5 - 15 \times 15$  m<sup>2</sup>. This range was selected based on empirical trial ranges commonly adopted in previous studies and aligned with the spatial resolution of the GNSS monitoring data. Grid units smaller than 5×5 m² were excluded due to data sparsity and increased susceptibility to noise, whereas larger units exceeding 15×15 m<sup>2</sup> tended to smooth out local deformation features, reducing sensitivity in classification. By using the method for determining the grid unit size considering displacement traction (see Section 1.1), the displacement data from 39 GNSS monitoring points with displacement attributes were obtained. The statistic of the distribution of the displacement directions in the four quadrants (I, II, III, and IV) is shown in Figure 6. The semisupervised learning for dataset expansion resulted in 6000 randomly generated unlabeled points, and then the labels of the 39 GNSS points were transferred to these points. This resulted in 6039 labeled samples with displacement attributes.

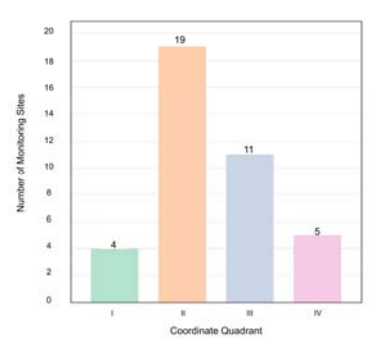


Fig. 6 Distribution of displacement trajectories for GNSS monitoring points

#### 3.2.2 Determination of the optimal grid unit size

Two constraints of data homogeneity and data volume should be considered when it comes to determine the optimal size of a grid unit. As previously noted, an optimal size was preliminarily determined to be  $5\times5$  -  $15\times15$  m<sup>2</sup>. The grid unit was then divided into  $5\times5$ ,  $6\times6$ ,  $7\times7$ ,  $8\times8$ ,  $9\times9$ ,  $11\times11$ ,  $13\times13$ , and  $15\times15$  m<sup>2</sup>, and the sample point data with displacement attributive labels expanded through semisupervised learning were superimposed and evaluated in terms of the consistency rate of the displacement directions in the different grid units across the 39 GNSS monitoring points, which was calculated as follows:

$$consistency = \frac{Max\{Class \ i \ sample \ size\}}{total \ sample \ size}$$

$$i \in (1, 2, 3, 4)$$
(2)

The distributions of the displacement directions associated with different grid unit sizes at the monitoring point 1 are shown in Figure 7. As shown in Figure 8 (the relationship between the consistency rate and grid unit size), the grid unit size at the inflection point is considered optimal because it ensures the data homogeneity within each unit while also controlling the overall data volume. Using an excessively small grid size would produce a very large number of grid units across the study area, increasing computational complexity and data redundancy. The relationships between the different grid unit sizes and the consistency rates for the monitoring points 1-10 are shown in Figures 9 and 10. The grid unit size of  $7\times7$ 

m<sup>2</sup> resulted in the smallest variations in consistency rates and therefore was considered to be the optimal size.

## 3.2.3 Assessment of sample dataset construction using ISSA-k-means clustering

To ensure the quality of the displacement-derived features, we calculated the number of days on which the displacement of each of the 39 monitoring points exceeded the average displacement across all points. In addition, cumulative displacement, average daily displacement, maximum daily displacement, and total monthly displacement were computed for each point from February to August 2017 (characterized by heavy rainfall). Features with a correlation greater than 0.85 (Figure 11) were excluded. Based on the extracted displacement-derived features, cluster analysis was performed using ISSA-k-means clustering to divide the landslide area into grid units. This clustering process grouped the assessment units into four distinct clusters according to similarities in their displacement characteristics. These clusters were then interpreted as four hazard levels: high, moderate, low, and very low. This unsupervised clustering approach provided a data-driven foundation for assigning risk levels to the units containing monitoring points, forming the initial labeled samples for subsequent semisupervised learning.

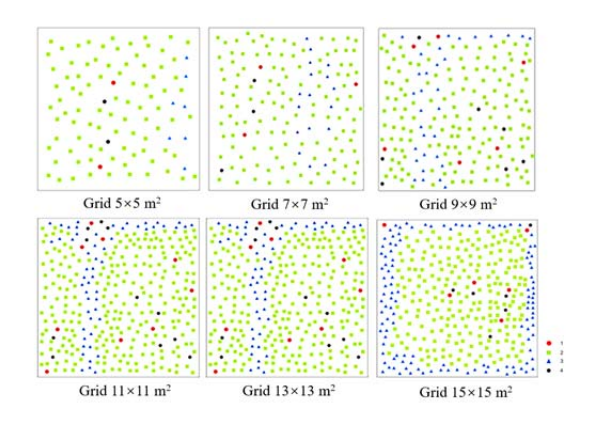


Fig. 7 Distribution of displacement directions in different grid unit sizes for monitoring point 1

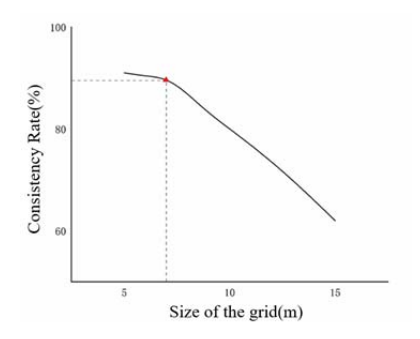


Fig. 8 Relationship between the consistency rate and grid unit size for point 1

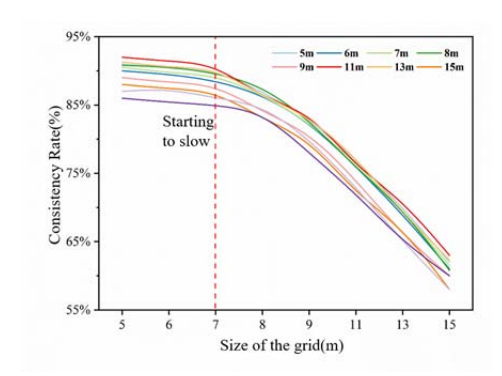


Fig. 9 Consistency rates of different grid unit sizes

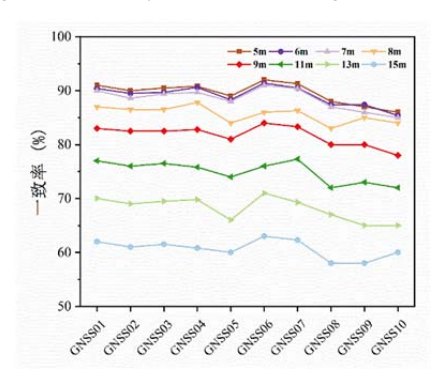


Fig. 10 Consistency rates for points 1-10

The assessment units containing the monitoring points were labeled accordingly, completing the preliminary construction of the assessment dataset. By using the semisupervised learning algorithm, the labels of the 39 labeled samples were spread to the randomly generated unlabeled samples. Finally, 500 labeled samples were obtained. Their distributions of the hazard levels, which met the requirements for model training, are shown in Figure 12.

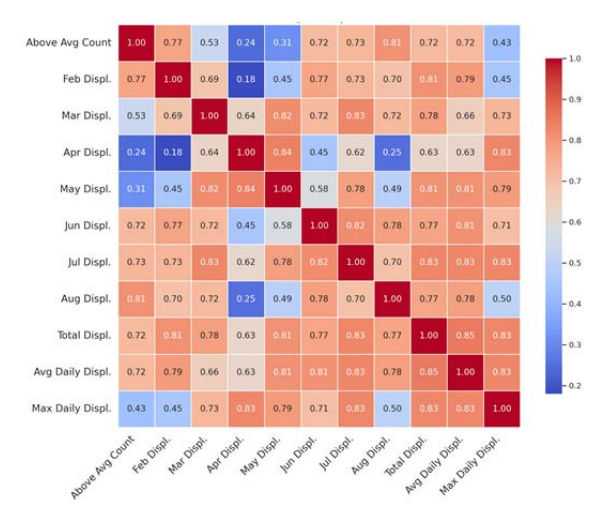


Fig. 11 Diagram of displacement feature correlations

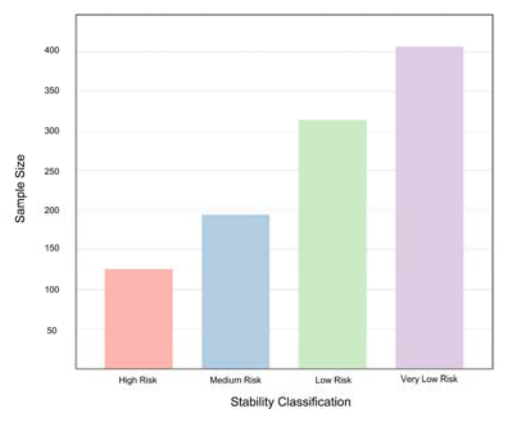


Fig. 12 Semisupervised classification of hazard levels

#### 3.2.4 Stacking model classification

#### (1) Influencing factor selection

The factors influencing landslide hazard levels were determined based on a comprehensive analysis of development characteristics and distribution patterns of landslides in the study area, including stratigraphic lithology, hydrology, engineering activities, and other factors. To determine the influencing factors, geological hazard data were used to the principles of systematicity, comparability, operability, difference, and combination of quantitative and qualitative indicators<sup>[25]</sup>. 11 factors were selected: surface roughness, topographic wetness index, topographic humidity index, elevation, distance from water bodies, distance from roads, distance from buildings, distance from geological structural cracks, lithology, slope angle and aspect (Figure 13).

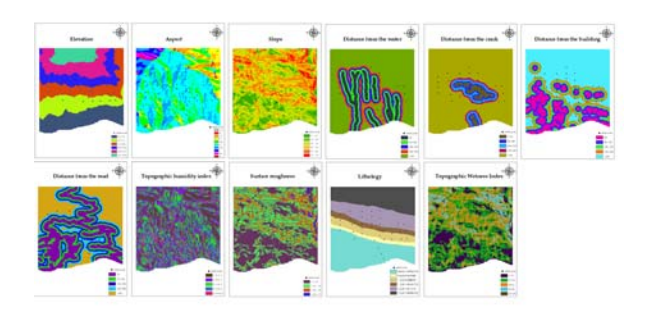


Fig. 13 Diagram of factors influencing landslide hazardousness

#### (2) Assessment model training

To avoid overfitting in the classification process, a two-layer stacking model was adopted. The first layer consisted of multiple base learners, including decision trees, support vector machines, logistic regression, and gradient boosting, each selected based on its distinct learning bias and proven performance in spatial classification tasks. The second layer was a meta-learner that integrated the outputs of the base models to make final predictions. The diversity of base classifiers introduces complementary perspectives—while some capture nonlinear boundaries, others generalize well under sparse conditions—thus enhancing robustness and reducing overfitting through error decorrelation.SVM, Gaussian Process, Random Forest, and XGBoost models were used as the first-level learners due to their high classification accuracies<sup>[26]</sup>. Moreover, various models were tested as meta-learners. Their accuracies on the training and test datasets are shown in Figure 14. The Decision Tree, Random Forest, AdaBoost, and bagging models showed overall overfitting when used as meta-learners. Therefore, a Logistic Regression model for its simplicity and high classification accuracy was selected as the meta-learner.

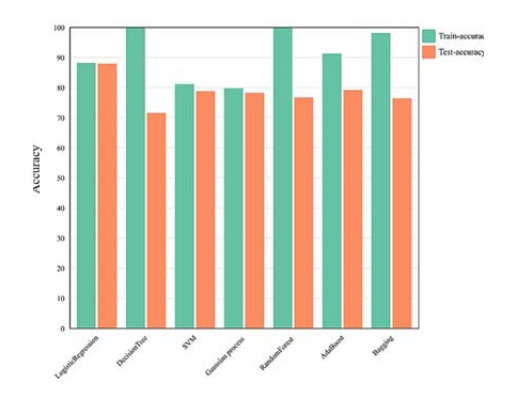


Fig. 14 Accuracy of different meta-learners

#### 4 Experimental results

#### 4.1 Comparison of various models' accuracies

To evaluate the impact of the grid unit size on the assessment accuracy, 500 labeled samples were divided into a training dataset and a test dataset in a 7:3 ratio, which ensured a good balance between the training and testing, and prevented overfitting while maintaining the sufficient test accuracy. The two datasets were then used to compare the stacking model's accuracy with the grid unit size determined by considering displacement traction  $(7 \times 7 \text{ m}^2)$  and that determined using the conventional grid unit size estimation formula (9×9 m<sup>2</sup>). The results are shown in Table 1. The model performance evaluated using standard was classification metrics including accuracy, F1 score, and Cohen's kappa coefficient, all derived from the confusion matrix<sup>[27]</sup>. The accuracy, F1 score, and kappa coefficient obtained using the  $7 \times 7$  m<sup>2</sup> grid unit size were 89.32%, 88.95%, and 82.78%, respectively, which were 2.15%, 1.30%, and 3.75% higher than those obtained using the  $9 \times 9$  m<sup>2</sup> grid unit size, respectively.

The ROC (Receiver Operating Characteristic) curves of the tested models were plotted with the false positive and true positive rates as their horizontal and vertical coordinates at different thresholds, and the corresponding AUC (Area Under Curve) values were given as well (Figure 15). As can be seen, the stacking model using the 7×7 m<sup>2</sup> grid unit size had the highest AUC (0.963) indicating the most reliable one<sup>[28,29]</sup>.

Table 1 Stacking model accuracy scores obtained using  $7\times7$  m<sup>2</sup> and  $9\times9$  m<sup>2</sup> grid unit sizes

Grid unit	Accuracy	F1 score	Kappa
size			coefficient
$7 \times 7 \text{ m}^2$	89.32%	88.95%	82.78%
$9 \times 9 \text{ m}^2$	87.17%	87.65%	79.03%

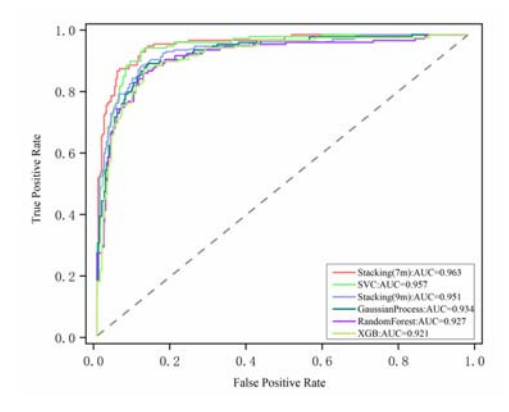


Fig. 15 ROC curves of the classification models

# 4.2 Comparison of the proposed landslide hazard levels assessment method's results with field data

To evaluate the reliability of this method, and thus its practicality to landslide disaster prevention and emergency responses, the results were compared with the actual landslide conditions in Guang'an (Figure 16). The landslides were divided into 13 areas: the source areas (SA 1-4), potential source areas (PSA 1-4), potential transportation areas (PTA 1–2), transportation areas (TA 1-2), and deposition area (DA)[30]. In line with the geological exploration and field investigation, the results obtained from the stacking model (transformed into raster data according to the classification labels) showed that the high hazard level was mainly distributed in SA 1-4, and TA, while the moderate hazard level was mainly distributed in PSA 1-4 and PTA 1-2 (Figure 17), indicating high prediction accuracy. The lower-left region in Figure 17, which contains the residential buildings, was identified as a potential impact area with predominantly high and moderate hazard level. Therefore, it was recommended to deploy additional GNSS monitoring points in this area, particularly in the zones exhibiting significant deformation, to enhance the spatial resolution of deformation monitoring and support more precise early warning and mitigation of potential landslide hazards.

In summary, the stacking method based on the grid unit size of  $7\times7$  m<sup>2</sup> produced the most accurate results than any other models, and the obtained distribution map of the landslide hazard levels was reliable. This method not only has the high theoretical accuracy but can also effectively guide the landslide disaster prevention and emergency responses.

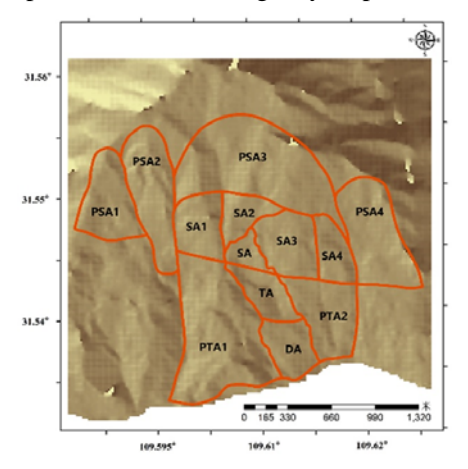


Fig. 16 Actual landslide -induced surface deformation profile

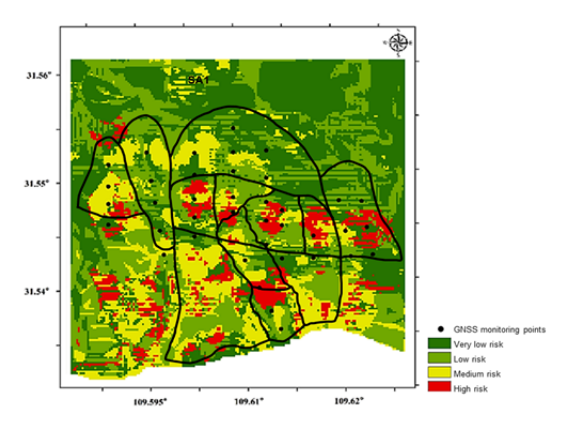


Fig. 17 Spatial distribution of landslide hazard levels ( $7 \times 7 \text{ m}^2$  grid unit size)

#### 5 Conclusions and Remarks

To address the complex issue of landslide hazard levels assessment, this study proposes an analytical method that considers the displacement traction effect.

The proposed method evaluates the correlations between characteristic displacements and uses ISSA–k-means clustering based on surface displacement data from monitoring points. This enables the construction of an assessment sample dataset by dividing a landslide into optimal grid units and determining their corresponding hazard levels. The method also employs a stacking model that considers 11 key influential landslide factors: surface roughness, topographic wetness index, topographic humidity index, elevation, distance from water bodies, distance from roads, distance from buildings, distance from geological structural cracks, lithology, slope angle and aspect.

Two main conclusions can be drawn from the conducted experiments. First, the proposed method outperforms the conventional grid-based approach in terms of accuracy and classification performance, demonstrating the effectiveness of the grid unit division strategy developed in this study for landslide hazard levels assessment. Second, the ISSA–k-means clustering can effectively establishes target regions, while the stacking model yields results that are highly consistent with the actual field data.

Overall, the proposed method is scientifically sound and practical as it provides a valuable reference for future research. To enhance the model's applicability and generalizability, future work could be focused on exploring migration learning to better adapt the model to various regional and typological needs and inform more effective decisions for disaster prevention and mitigation.

Acknowledgement: The research was partially funded by Chongqing Technical Innovation and Application Development Special Key Project: Research on Key Technologies for Safety Pre-warning of Mountain Transportation Infrastructure Structure (CSTB2022TIAD-KPX0098).

#### References

[1] FENG S. (2021): Study on the ability improvement of emergency rescue social organizations under the background of risk society [C]//Proceedings of 3rd

- International Symposium on Education, Culture and Social Sciences (ECSS 2021), Eds., Department of Law and Political Science, North China Electric Power University (Baoding), 2021: 325-328.
- [2] LI R. (2022): Research on landslide stability evaluation method considering multiple factors [D]. Chongqing: Chongqing Jiaotong University, 2022. (in Chinese)
- [3] XU Y X, HU Q W, DUAN Y S, et al. (2024): Landslide dynamic monitoring technology by integrating LiDAR point cloud and UAV image [J]. Bulletin of Surveying and Mapping, 2024(8): 42-47. (in Chinese)
- [4] SU X J, ZHANG Y, MENG X M, et al. (2024): Early identification and development characteristics analysis of potential landslides in the Huanza section of the China-Pakistan Economic Corridor using SBAS-InSAR [J]. Journal of Remote Sensing, 2024, 28(4): 885-899.
- [5] LI M H, ZHANG L, DONG J, et al. (2021): Detection and monitoring of potential landslides along Minjiang River valley in Maoxian County, Sichuan using radar remote sensing [J]. Geomatics and Information Science of Wuhan University, 2021, 46(10): 1529-1537.
- [6] Süzen, M. L., & Doyuran, V. (2004): A comparison of the GIS based landslide susceptibility assessment methods: multivariate versus bivariate. Environmental Geology, 45(5), 665–679.
- [7] Reichenbach, P., Rossi, M., Malamud, B. D., Mihir, M., & Guzzetti, F. (2018): A review of statistically-based landslide susceptibility models. *Earth-Science Reviews*, 180, 60–91.
- [8] LI J, et al. (2003): Analysis of grid size selection in landslide risk evaluation methods based on raster GIS [J]. Journal of Remote Sensing, 2003, 7(2): 86-93.
- [9] FELL R, COROMINAS J, BONNARD C, et al. (2008): Guidelines for landslide susceptibility, hazard and risk zoning for land use planning [J]. Engineering Geology, 2008, 102(3/4): 85-98.
- [10] ZÊZERE J L, PEREIRA S, MELO R, et al. (2017): Mapping landslide susceptibility using data-driven methods [J]. Science of The Total Environment,

- 2017, 589: 250-267.
- [11] THIEBES B, BELL R, GLADE T, et al. (2010): Landslide early warning models - Five applications within the ILEWS project [J]. EGU General Assembly Conference Abstracts, 2010.
- [12] WANG N, GUO Y, LIU T. (2019): Landslide risk assessment based on support vector machine model [J]. Science, Technology and Engineering, 2019, 19: 70-78.
- [13] ZHOU F. Research on early intelligent discrimination of landslide stability and fuzzy comprehensive prediction of hazards in the reservoir area of Coronation Hydropower Station [D]. Changchun: Jilin University, 2013.
- [14] PRADHAN B, LEE S. (2010): Landslide susceptibility assessment and factor effect analysis: backpropagation artificial neural networks and their comparison with frequency ratio and bivariate logistic regression modelling [J]. Environmental Modelling & Software, 2010, 25(6): 747-759.
- [15] LIN S, ZHENG H, HAN C, et al. (2021): Evaluation and prediction of slope stability using machine learning approaches [J]. Frontiers of Structural and Civil Engineering, 2021, 15(4): 821-833.
- [16] LI X F, NISHIO M, SUGAWARA K, et al. (2024): Enhancing prediction of landslide dam stability through AI models: A comparative study with traditional approaches [J]. Geomorphology, 2024, 454: 109120.
- [17] ZHAO Q, WANG H, ZHOU H Y, et al. (2024): An interpretable and high-precision method for predicting landslide displacement using evolutionary attention mechanism [J]. Natural Hazards, 2024, 120(13): 11943-11967.
- [18] LI J. (2003): Analysis of grid size selection in landslide risk assessment method based on GIS [J]. Journal of Remote Sensing, 2003, 7: 86-93.
- [19] LEI T Q, LI S Q. (2021): Improved K-means clustering algorithm by combining with multiple factors [C]//2021 3rd International Conference on Advances in Computer Technology, Information Science and Communication (CTISC). April 23-25, 2021. Shanghai, China. IEEE, 2021: 258-263.

- [20] CHEN Y R, ZHOU J, HE X S, et al. (2024): An improved density peaks clustering based on sparrow search algorithm [J]. Cluster Computing, 2024, 27(8): 11017-11037.
- [21] DENG N, LI Y, CUI Y. (2022): Landslide susceptibility assessment based on machine learning hybrid model [J]. Science, Technology and Engineering, 2022, 22: 5539-5547.
- [22] CHEN W, POURGHASEMI H R, PANAHI M, et al. (2017): Spatial prediction of landslide susceptibility using an adaptive neuro-fuzzy inference system combined with frequency ratio, generalized additive model, and support vector machine techniques [J]. Geomorphology, 2017, 297: 69-85.
- [23] YANG W T, NIU R Q, SI R J, et al. (2024): Geological hazard susceptibility analysis and developmental characteristics based on slope unit, using the Xinxian County, Henan Province as an example [J]. Sensors, 2024, 24(8): 2457.
- [24] LI X, XUE G C, XIA N, et al. (2023): Geological hazard susceptibility evaluation based on CF, CF-LR and CF-AHP models in National Tropical Rain Forest Park: Taking Baoting County, Hainan Province as an example [D]. Modern Geology, 2023, 37: 1033-1043.
- [25] DUAN Q W. (2021): Personal credit risk assessment based on Stacking fusion model [D] Jinan: Shandong University, 2021.
- [26] Cui Y Y. (2021): A comparative study on evalution methods of landslide susceptibility based on different evaluation units: A case study of Luonan County, Shaanxi Province [D]. Xi'an: Xi'an University of Science and Technology, 2021.
- [27] Sokolova, M., & Lapalme, G. (2009): A systematic analysis of performance measures for classification tasks. Information Processing & Management, 45(4), 427–437. https://doi.org/10.1016/j.ipm.2009.03.002
- [28] ZHU X B, BI Y G, DU J M, et al. (2023): Research on deep learning method recognition and a classification model of grassland grass species based on unmanned aerial vehicle hyperspectral remote sensing [J]. Grassland Science, 2023, 69(1): 3-11.
- [29] HUANG S, TU X, ZHOU S. (2022): Application of

- Kappa coefficient in the consistency evaluation of color fastness, Knitting Industry, 2022: 71-75.
- [30] WANG L Q, YIN Y P, HUANG B L, et al. (2019): Formation and characteristics of Guang'an Village landslide in Wuxi, Chongqing, China [J]. Landslides, 2019, 16(1): 127-138.

#### Authors



**Xingchi Chen is a** postgraduate student at the School of Smart City, Chongqing Jiaotong University, Chongqing, China, research interest: landslide extraction, landslide susceptibility mapping.



Yuzhi Meng received her BSc. in Geomatics from Xi'an University of Science and Technology, China, in 2022 and is currently pursuing her MSc. degree in Surveying and Mapping Science and Technology at Chongqing Jiaotong University,



China. Her research interests include Landslide hazard monitoring and landslide risk analysis.

**Junzhe Zhou** received his BSc. degree from Hefei University of Technology, China, in 2021, and is

currently pursuing his MSc. degree in Surveying and Mapping Science and Technology at Chongqing Jiaotong University, China. His research focuses include landslide displacement prediction and landslide risk analysis.

**Yutao Zhou** works in the field of surveying and mapping, where he focuses on applied research and practice.

**Zhengdong Leng** is engaged in surveying and mapping studies, and he contributes to the development of geospatial applications.

**Kun** Wang works in surveying and mapping. He is involved in both research and practical implementation.